Role of the C-Terminus of the High-Conductance Calcium-Activated Potassium Channel in Channel Structure and Function

William A. Schmalhofer,[‡] Manuel Sanchez,[‡] Ge Dai,[‡] Ashvin Dewan,[‡] Lorena Secades,[‡] Markus Hanner,[‡] Hans-Guenther Knaus,[§] Owen B. McManus,[‡] Martin Kohler,[‡] Gregory J. Kaczorowski,[‡] and Maria L. Garcia*[,‡]

Department of Ion Channels, Merck Research Laboratories, P.O. Box 2000, Rahway, New Jersey 07065, and Institute for Biochemical Pharmacology, Peter Mayr Strasse 1, A-6020 Innsbruck, Austria

Received March 22, 2005; Revised Manuscript Received June 3, 2005

ABSTRACT: The role of ion channels in cell physiology is regulated by processes occurring after protein biosynthesis, which are critical for both channel function and targeting of channels to appropriate cell compartments. Here we apply biochemical and electrophysiological methods to investigate the role of the high-conductance, calcium-activated potassium (Maxi-K) channel C-terminal domain in channel tetramerization, association with the β1 subunit, trafficking of the channel complex to the cell surface, and channel function. No evidence for channel tetramerization, cell surface expression, or function was observed with Maxi-K_{1-323}, a construct truncated three residues after the S_6 transmembrane domain. However, Maxi-K_{1-343} and Maxi-K_{1-441} are able to form tetramers and to associate with the β1 subunit. Maxi-K_{1-343}−β1 and Maxi-K_{1-441}−β1 complexes are efficiently targeted to the cell surface and cannot be pharmacologically distinguished from full-length channels in binding experiments but do not form functional channels. Maxi-K_{1-651} forms tetramers and associates with β1; however, the complex is not present at the cell surface, but is retained intracellularly. Maxi-K_{1-651} surface expression and channel function can be fully rescued after coexpression with its C-terminal complement, Maxi-$K_{652-1113}$. However coexpression of Maxi-K_{1-343} and Maxi-K_{1-441} with their respective C-terminal complements did not rescue channel function. Together, these data demonstrate that the domain(s) in the Maxi-K channel necessary for formation of tetramers, coassembly with the β1 subunit, and cell surface expression resides within the S_0−S_6 linker domain of the protein, and that structural constraints within the gating ring in the C-terminal region can regulate trafficking and function of constructs truncated in this region.

Potassium channels play important roles in physiology through regulation of many critical cellular functions, including electrical properties of neurons, muscle contraction, hormone and neurotransmitter release, electrolyte movement, and proliferation (*1*). Following gene transcription, numerous mechanisms exist that contribute to regulating levels of functional channels in the cell. A number of diseases result from mutations that alter channel trafficking, causing the protein to be retained in intracellular organelles and not reach the cell surface (*2*−*4*). In the human ether-a-go-go related gene, defects in trafficking contribute to human hereditary long QT syndrome, a cardiac disease that increases susceptibility to ventricular arrhythmias and sudden cardiac death (*5*).

High-conductance, calcium-activated potassium (Maxi-K)[1] channels play an important role in regulating smooth muscle contractility (*6*). In addition to the pore-forming subunit, Slo1, smooth muscle Maxi-K channels also contain an auxiliary β1 subunit present in a 1:1 stoichiometry within an octameric complex. β1 alters the calcium sensitivity of the channel by shifting its calcium-dependent midpoint of activation to more hyperpolarized potentials (*7*). In addition, some pharmacological properties of the channel are also modified by the presence of β1 (*7*, *8*). Two features distinguish Slo1 from other potassium channels: (1) an extracellular N-terminus of the protein (*9*) and (2) a large cytoplasmic, C-terminal domain which controls different functional properties of the channel. In this region, two regulators of potassium conductance (RCK) domains have been identified on each α subunit that are connected to the pore region by a short linker (*10*−*12*). The RCK domains have been proposed to form a gating ring, where calcium binding causes a conformational change that promotes channel opening by pulling the linker connecting the gating ring to the pore region. In addition to this functional role, three different studies have also proposed a role for the C-terminal region of Slo1 in both channel tetramerization and cell surface expression. A region of ∼163 amino acids, BK-T1, located after S_6 and containing the first putative RCK domain, was reported to be critical in the assembly of functional tetrameric channels (*13*), and in other studies, the cytoplasmic tail has been postulated to be involved in cell

* To whom correspondence should be addressed. Phone: (732) 594-7564. Fax: (732) 594-3925. E-mail: maria_garcia@merck.com.

[‡] Merck Research Laboratories.

[§] Institute for Biochemical Pharmacology.

[1] Abbreviations: Maxi-K, high-conductance, calcium-activated potassium channel; Slo1, pore-forming subunit of the Maxi-K channel; RCK, regulator of potassium conductance; ChTX, charybdotoxin; IbTX, iberiotoxin; [^{125}I]IbTX-D19Y/Y36F, monoiodotyrosine iberiotoxin-D19Y/Y36F; K_d, equilibrium dissociation constant; K_i, equilibrium inhibition constant; k_{-1}, dissociation rate constant; DSS, disuccinimidyl suberate; ER, endoplasmic reticulum.

10.1021/bi050527u CCC: $30.25
Published on Web 07/07/2005

surface expression and apical localization (*14*−*16*). However, data from another study conflict with these observations, since a truncated Maxi-K channel lacking the entire intracellular C-terminus was shown to form channels with the same characteristics as full-length Slo1 (*17*). These later data would suggest that the C-terminal region of the pore-forming subunit of the Maxi-K channel is not necessary for subunit association or tetramerization, cell surface expression, or calcium sensitivity. This study attempts to clarify inconsistencies in these past reports.

In the study presented here, the role of the cytoplasmic C-terminal region of hSlo1 in subunit tetramerization and cell surface expression was directly evaluated by determining the ability of different C-terminally truncated mutants to bind iberiotoxin (IbTX), a selective Maxi-K channel blocker, and to recognize an antibody directed against the extracellular, N-terminal region of hSlo1. In addition, association of Maxi-K channel constructs with β1 was studied using cross-linking experiments with radiolabeled IbTX, and electrophysiological recordings were carried out to determine the functional consequences of the truncations. Results from these experiments indicate that the entire C-terminal region beginning at the first RCK domain, although important for channel function, is not necessary for channel tetramerization, cell surface expression, or association with β1, but truncation of the linker after S_6 significantly alters the properties of the protein. Trafficking to the cell surface of constructs that extend beyond residue 343 appears to depend on certain conformations of the gating ring.

EXPERIMENTAL PROCEDURES

Materials. Restriction enzymes and the pCI-neo vector were bought from Promega. The pEGFP-N1 vector was from Clontech, and *Pfu* DNA polymerase was from Stratagene. Alexa-Fluor546 goat anti-rabbit IgG (H+L) was obtained from Molecular Probes. Horseradish peroxidase-conjugated donkey anti-rabbit Ig and the ECL-plus Western blot detection system were bought from Amersham Biosciences. TsA-201 cells were a gift of R. DuBridge. Paxilline was from Sigma, IbTX from Peptides International, recombinant *N*-glycanase from Genzyme, and the FuGENE6 transfection reagent from Roche. Iberiotoxin-D19Y/Y36F (IbTX-D19Y/Y36F) was prepared and radioiodinated as described previously (*18*), and Alexa-Fluor488-IbTX was prepared as described previously (*19*). All other reagents were obtained from commercial sources and were of the highest purity commercially available.

Mutant Channel Constructs. Constructs of hSlo1 [KCNMA1, K_{Ca}1.1, U11058 (*20*)] with different C-terminal deletions were generated. All truncated α subunits had in common the N-terminus−S_6 region of the protein. For Maxi-K_{1-343}, Maxi-K_{1-441}, and Maxi-K_{1-651}, the corresponding C-terminal regions, Maxi-$K_{344-1113}$, Maxi-$K_{442-1113}$, and Maxi-$K_{652-1113}$, respectively, were also subcloned. Constructs were made by including appropriate restriction enzyme recognition sites into the PCR primers. PCR amplification was carried out using proofreading *Pfu* DNA polymerase. Amino acid sequences of the constructs (restriction sites used for cloning into pCI-neo are given in brackets) are as follows: Maxi-K_{1-323}, Met_1−Ile_{323} (MluI, NotI); Maxi-K_{1-343}, Met_1−Lys_{343} (MluI, NotI); Maxi-$K_{344-1113}$, His_{344}−Leu_{1113} (EcoRI, NotI); Maxi-K_{1-441}, Met_1−Ile_{441} (SalI, NotI); Maxi-K_{1-651}, Met_1−Gly_{651} (SalI, NotI); and Maxi-$K_{652-1113}$, Met_{652}−Leu_{1113} (XbaI, NotI). The integrity of the constructs was verified by nucleotide sequencing (automated DNA sequencer, ABI 377). Maxi-K_{1-323} used in this study contains Ala at position 86, whereas Val is the corresponding residue in the mouse clone (*17*). The bovine β1 subunit (KCNMB1) has been previously described (*8*).

Transfection of TsA-201 Cells and Membrane Preparation. Procedures for handling TsA-201 cells, their transfection with FuGENE6, and preparation of membrane vesicles have been previously described (*21*). For electrophysiological recordings, 35 mm polystyrene Petri dishes containing 3 mm × 3 mm poly-D-lysine-treated glass chips were seeded 24 h after transfection with ∼20000 cells which were allowed to attach for ∼18 h at 37 °C.

[^{125}I]IbTX-D19Y/Y36F Binding. The interaction of [^{125}I]-IbTX-D19Y/Y36F with TsA-201 membranes was assessed in a medium consisting of 10 mM NaCl, 20 mM Tris-HCl (pH 7.4), and 0.1% bovine serum albumin. For saturation experiments, membranes were incubated with increasing concentrations of [^{125}I]IbTX-D19Y/Y36F, in a total volume of 0.5 mL, for 20 h at room temperature, and triplicate samples were obtained for each experimental point. Competition experiments were carried out with [^{125}I]IbTX-D19Y/Y36F in the absence or presence of increasing concentrations of the test compound. Nonspecific binding was defined in the presence of 10 nM IbTX. Separation of bound from free ligand was achieved using filtration protocols as described previously (*18*). For binding to cells, poly-D-lysine plates were seeded at a density of 40000 cells per well, and cells were allowed to attach for approximately 18 h at 37 °C. [^{125}I]-IbTX-D19Y/Y36F was added to wells, and incubation took place under the same growth conditions. Competition experiments were carried out in the absence or presence of increasing concentrations of the test compound for 20 h, and quadruplicate samples were run for each experimental point. Nonspecific binding was defined in the presence of 200 nM IbTX. At end of incubation, cells were washed with 200 μL of Dulbecco's phosphate-buffered saline (D-PBS) twice to separate bound from free ligand, and radioactivity associated with cells was determined using a Packard Top-count liquid scintillation counter. Data from saturation, competition, and ligand dissociation experiments were analyzed as described previously (*8*).

Alexa-Fluor488-IbTX Binding. Cells were seeded into Lab-Tek (HEK293) or culture slides (TsA201), at a density of 10000 cells per chamber, and allowed to attach for approximately 18 h at 37 °C. Growth medium was aspirated, and solutions containing Alexa-Fluor488-IbTX were added to the chambers. Incubations took place for approximately 24 h, in the dark, at 37 °C. At the end of incubation, the medium was aspirated, and chambers were washed twice with D-PBS. Images were obtained using either a Nikon TE300 instrument equipped with a 175 W xenon arc lamp and 403 ± 7 and 515 ± 15 nm filters (TsA-201 cells) or a Zeiss LSM410 confocal imaging system with an argon laser tuned to 488 nm as the excitation source, and 535/50 BP as the emission filter (HEK293 cells).

Cross-Linking Experiments. Covalent incorporation of [^{125}I]IbTX-D19Y/Y36F into membranes in the presence of the bifunctional cross-linking reagent, disuccinimidyl sub-

erate (DSS), was carried out essentially as described previously (*22*). Samples were subjected to SDS−PAGE, and gels were dried and exposed to CL-X Posure film.

Immunoblot Analysis. After SDS−PAGE, proteins were transferred onto polyvinylidene diflouride membranes. Membranes were incubated in 10% skim milk powder, 0.1% Tween 20, and 0.5% Triton X-100 in TBS [150 mM NaCl and 20 mM Tris-HCl (pH 7.4)] overnight at 4 °C and then with affinity-purified polyclonal serum raised against residues 28−40 of hSlo1 (α28−40) (*23*) for 4 h at 22 °C. After several washes in 0.1% Tween 20 and 0.5% Triton X-100 in TBS, horseradish peroxidase-conjugated donkey anti-rabbit Ig was added at a 1:5000 dilution and blots were incubated for 60 min at 22 °C. Membranes were washed as before and developed in the ECL-plus Western blot detection system following the manufacturer's protocol.

Immunocytochemistry. Cells were seeded into culture slides at a density of 10000 cells per chamber and allowed to attach for approximately 18 h at 37 °C. For colocalization experiments, TsA-201 cells were cotransfected with pECFP-ER. Cells were fixed with 4% formaldehyde for 15 min at room temperature and then washed for 10 min, twice, with or without 0.2% Triton X-100. Nonspecific sites were blocked by incubation with 5% normal goat serum for 120 min at room temperature. Blocking buffer was removed, and cells were incubated overnight at room temperature with crude α28−40 antibody diluted 1:1200 in 0.1% bovine serum albumin. After incubation, cells were washed four times, for 10 min each, and then incubated with Alexa-Fluor546 goat anti-rabbit IgG diluted 1:4000 for 2 h at room temperature. Cells were washed; chamber walls were removed, and slides were sealed with a #1 coverslips. Images were obtained on a Nikon TE300 instrument (TsA-201 cells) with a 175 W xenon arc lamp with either 555 ± 12.5 and 605 ± 20 nm filters (Alexa-Fluor546) or 440 ± 21 and 480ALP nm filters (pECFP-ER) or a Zeiss LSM410 confocal imaging system with an argon laser tuned to 488 nm as the excitation source, and 535/50 BP as the emission filter (HEK293 cells).

Electrophysiological Recordings. TsA-201 cells transfected with Maxi-K channel constructs along with a plasmid encoding green fluorescent protein to facilitate identification of transfected cells were seeded on glass coverslips. Recordings were carried out 1−3 days after transfection using standard on-cell, whole-cell, or inside-out configurations of the patch-clamp technique (*24*) with a HEKA EPC9 amplifier controlled by PULSE software (HEKA Elektronik, Lambrecht, Germany). Currents were digitized at 10 kHz and digitally filtered at 3 kHz. No corrections for junction potentials were used. Whole-cell and inside-out configurations were used to study voltage- and calcium-dependent channel gating. Currents were activated by ramp or step changes in membrane potential. Voltage ramps with a duration of 1 s from −100 to 180 mV were applied from negative holding potentials (from −60 to −100 mV) to give an initial estimate of channel expression and gating. Conductance−voltage curves were calculated from initial tail current amplitudes at −100 mV following 100 ms voltage steps (from −100 to 180 mV) applied every 5 s from a holding potential of −80 mV. For whole-cell recordings, the pipet solution contained 150 mM KCl, 0.01 mM $CaCl_2$, and 10 mM HEPES (pH adjusted to 7.2 with KOH), and the external solution contained 160 mM NaCl, 4.5 mM KCl, 1.8 mM $CaCl_2$, 1 mM $MgCl_2$, and 10 mM HEPES (pH 7.2) with NaOH. For inside-out recordings, the pipet solution contained 150 mM KCl, 0.01 mM $CaCl_2$, 1 mM $MgCl_2$, and 10 mM HEPES (pH adjusted to 7.2 with KOH). To examine voltage-dependent channel gating of expressed channels, a buffered calcium (1 μM) solution containing 150 mM KCl, 5 mM EGTA, 4.19 mM $CaCl_2$, and 10 HEPES (pH adjusted to 7.2 with KOH) was used. Solutions used to examine calcium sensitivity of channel gating contained 150 mM KCl, 0.01−1 mM $CaCl_2$, and 10 mM HEPES (pH adjusted to 7.2 with KOH). A nominally calcium-free solution contained 150 mM KCl, 1 mM EGTA, and 10 mM Hepes (pH adjusted to 7.2 with KOH). Solutions were continuously applied to the experimental chamber (0.2−0.3 mL volume) by gravity-driven perfusion at 1−2 mL/min. Current amplitudes were measured with PULSEFIT software (HEKA Elektronik) and plotted using IGOR software (Wavemetrics, Lake Oswego, OR). The voltage dependence of channel activation was estimated by fitting the initial tail current amplitudes to the Boltzmann function; $I(V) = I_{max}/\{1 + \exp[-(V_m - V_{1/2})/k]\}$, where I_{max} is the maximal current, $V_{1/2}$ is the half-activation voltage, and k is the slope factor. Results are expressed as mean ± the standard error of mean (SEM) of, at least, seven experiments. All experiments were carried out at room temperature (22−25 °C).

RESULTS

Role of the C-Terminus in Binding of [^{125}I]IbTX-D19Y/Y37F to Maxi-K Channels. Two features distinguish the pore-forming subunit of Maxi-K channels, hSlo1, from other members of the potassium channel superfamily: (1) an extracellular N-terminus of the channel protein (*9*) and (2) the existence of a large intracellular C-terminal region that contains two RCK domains connected to the pore region by a short linker (*10*−*12*). Although several studies have attempted to define the role of the Maxi-K C-terminal domain in channel structure, cell surface expression, and function (*13*−*16*, *25*−*28*), the report that a protein truncated at position 323, right after S_6, was able to form channels with characteristics similar to the those of the full-length protein (*17*) has brought controversy to the understanding of Maxi-K channel structure and function. Given this conundrum, we determined the role of the C-terminus of the Maxi-K channel in channel tetramerization by evaluating the binding characteristics of the selective Maxi-K channel peptide blocker, [^{125}I]IbTX-D19Y/Y36F (*18*), with different Maxi-K channel constructs.

Four Maxi-K constructs with different deletions at the C-terminus, as well as the wild-type channel, were used in these studies (Figure 1A). These constructs are intended to contain selected regions of proposed functional relevance, including the pore-RCK1 linker, and the RCK domains. Maxi-K_{1-323} is identical to the construct previously used by others (*14*, *17*), but with Ala substituted for Val at position 86 (*17*). Maxi-K_{1-343} extends 22 amino acids beyond S_6, contains the linker, and ends before the beginning of RCK1. Maxi-K_{1-441} is truncated within RCK1. Maxi-K_{1-651} contains the entire RCK1 domain, but not the RCK2 domain. Each of these constructs was transiently cotransfected with the β1 subunit of the channel in TsA-201 cells, and membranes were prepared and characterized by immunostaining and pharmacological techniques. Western blots using an antibody raised

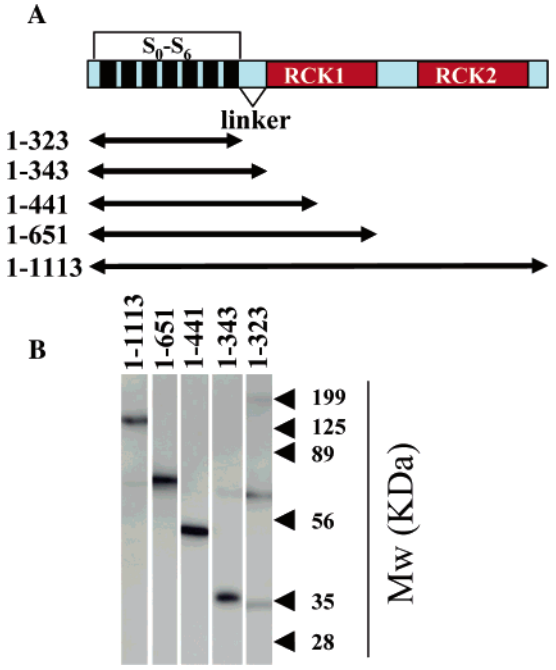

FIGURE 1: Maxi-K channel constructs. (A) Schematic representation of one of the four α subunits of the Maxi-K channel tetramer showing the transmembrane S_0-S_6 segments, linker region, and the intracellular RCK domains. The C-terminally truncated mutants used in this study, Maxi-K_{1-323}, Maxi-K_{1-343}, Maxi-K_{1-441}, and Maxi-K_{1-651}, are illustrated. (B) Western blots after SDS−PAGE of membranes prepared from TsA-201 cells transiently transfected with either the full-length Maxi-K channel or the different C-terminally truncated Maxi-K constructs. Blots were probed with an antibody raised against the N-terminal region of the Maxi-K channel. Specific immunostaining signals with appropriate characteristics for each construct were observed. Note that for Maxi-K_{1-323}, two specific immunostaining signals were consistently observed. The higher-molecular weight band most likely represents a dimer of a single Maxi-K_{1-323} subunit.

against the N-terminal region of the channel indicated the presence of specific immunostaining signals with characteristics appropriate for each construct (Figure 1B). In the case of Maxi-K_{1-323}, two specific immunostaining signals were consistently observed. The most likely explanation is that the larger molecular weight band represents the association of two monomeric subunits. Binding of the selective Maxi-K channel blocker [^{125}I]IbTX-D19Y/Y36F (*18*) to these membrane preparations was evaluated, and results of saturation experiments are presented in Figure 2A−D. Binding of [^{125}I]-IbTX-D19Y/Y36F occurs to a single class of sites in Maxi-K_{1-343}, Maxi-K_{1-441}, and Maxi-K_{1-651} membranes that display K_d values of 6.0 ± 0.8 (n = 8), 8.2 ± 0.4 (n = 3), and 9.1 ± 1.7 pM (n = 5) for the radiolabeled peptide, respectively. Importantly, these values are within the range of those observed with the full-length Maxi-K channel, which is 6.5 ± 0.1 pM (n = 3). Since the high-affinity interaction of pore-blocking peptides, such as IbTX, requires the channel's tetrameric structure (*29*), these data suggest that the C-terminal region of the Maxi-K channel that contains the RCK domains is not necessary for channel tetramerization. [^{125}I]-IbTX-D19Y/Y36F was not seen to bind to Maxi-K_{1-323} despite the presence of the protein in Western blots. These data indicate either a lack of tetramerization with this construct or a significant change in the architecture of the outer vestibule of the channel where this peptide probe binds.

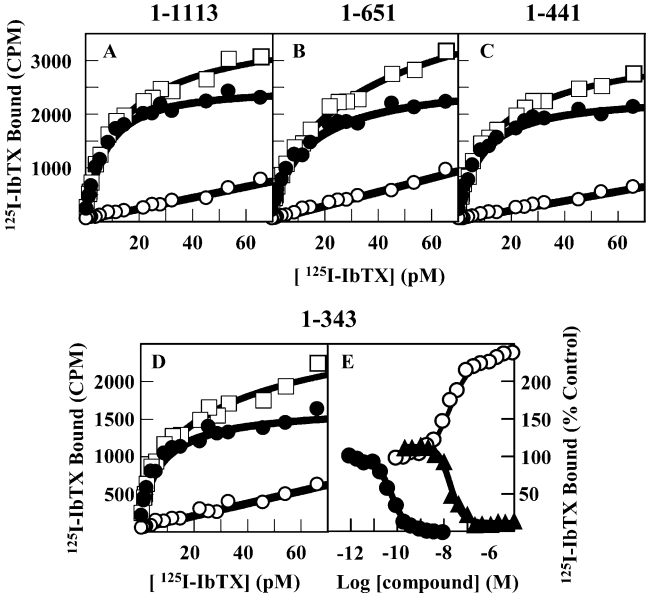

FIGURE 2: Binding of [^{125}I]IbTX-D19Y/Y36F to Maxi-K channels. Role of the C-terminus. Membranes prepared from TsA-201 cells transiently transfected with the β1 subunit and either Maxi-K_{1-1113} (A), Maxi-K_{1-651} (B), Maxi-K_{1-441} (C), or Maxi-K_{1-343} (D) were incubated with increasing concentrations of [^{125}I]IbTX-D19Y/Y36F, for ~20 h at room temperature. Separation of bound from free ligand was carried out by filtration techniques, as described in Experimental Procedures. Total binding (□), nonspecific binding (○), determined in the presence of 10 nM IbTX, and specific binding (●), defined as the difference between total and nonspecific binding, are presented. Specific binding is a saturable function of [^{125}I]IbTX-D19Y/Y36F concentration and displays K_d values of 6.0 ± 0.8 (n = 8), 8.2 ± 0.4 (n = 3), 9.1 ± 1.7 (n = 5), and 6.5 ± 0.1 pM (n = 3) for Maxi-K_{1-343}, Maxi-K_{1-441}, Maxi-K_{1-651}, and Maxi-K_{1-1113}, respectively. In transfections with Maxi-K_{1-323}, specific [^{125}I]IbTX-D19Y/Y36F binding was not detected. (E) Membranes prepared from TsA-201 cells transiently transfected with Maxi-K_{1-343} and β1 were incubated with ~3 pM [^{125}I]IbTX-D19Y/Y36F in the absence or presence of increasing concentrations of IbTX (●), paxilline (○), or penitrem A (▲) until equilibrium was achieved. Specific binding data are presented relative to an untreated control.

Binding of [^{125}I]IbTX-D19Y/Y36F to the Maxi-K constructs was characterized in further detail. As expected, unlabeled IbTX inhibited binding of [^{125}I]IbTX-D19Y/Y36F to all the constructs with similar K_i values (Figure 2E and data not shown), and kinetics of [^{125}I]IbTX-D19Y/Y36F dissociation followed monoexponential decays, indicative of a first-order reaction, with $t_{1/2}$'s of 156, 182, 190, and 445 min for Maxi-K_{1-343}, Maxi-K_{1-441}, Maxi-K_{1-651}, and the full-length protein, respectively (data not shown). In addition, for all the constructs, the indole diterpenes paxilline and penitrem A displayed the characteristic positive allosteric enhancing or inhibitory behavior on [^{125}I]IbTX-D19Y/Y36F binding that was previously reported for the full-length channel (Figure 2E and data not shown) (*8*, *30*). Even in the presence of paxilline, binding of [^{125}I]IbTX-D19Y/Y36F to Maxi-K_{1-323} was never observed. All these data, taken together, strongly suggest that the pharmacological properties of Maxi-K channels with respect to pore-blocking peptides and indole diterpene inhibitor interactions reside within the S_0-S_6 linker region of the channel, and they also provide evidence that other regions of the protein, in addition to the outer vestibule where pore-blocking peptides bind, must be properly folded.

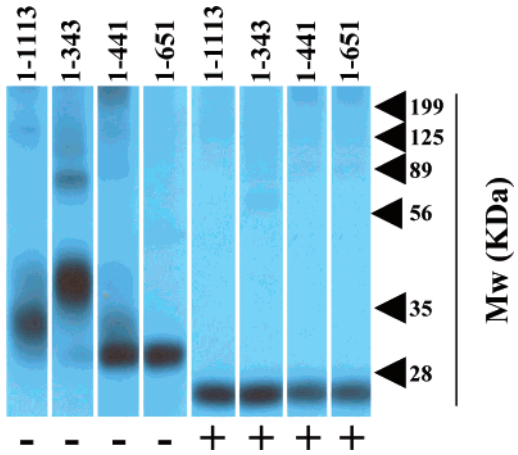

FIGURE 3: Cross-linking of [^{125}I]IbTX-D19Y/Y36F to the β1 subunit of the Maxi-K channel. Membranes prepared from TsA-201 cells transiently transfected with the β1 subunit and either Maxi-K_{1-1113}, Maxi-K_{1-343}, Maxi-K_{1-441}, or Maxi-K_{1-651} were incubated with ~40 pM [^{125}I]IbTX-D19Y/Y36F, reacted with DSS, and subjected to SDS−PAGE as described in Experimental Procedures. The migration of molecular weight standards is indicated by arrows. Control samples (−) and samples incubated with recombinant *N*-glycanase (+) for 18 h at 37 °C are illustrated.

Association of α *and* β*1 Subunits of the Maxi-K Channel*. In addition to the pore-forming subunit, native Maxi-K channels contain a β subunit that can alter the biophysical and pharmacological properties of the resulting complex. Four different β subunits have been identified, and β1 appears to be almost exclusively associated with the channel in smooth muscle (*6*, *31*). To determine if the Maxi-K channel constructs previously characterized are able to associate with β1, cross-linking experiments were carried out in the presence of the bifunctional reagent DSS, after binding of [^{125}I]IbTX-D19Y/Y36F to the respective membranes. For all constructs, covalent incorporation of radioactivity into the β1 subunit of the channel occurred and treatment of the preparations with *N*-glycanase resulted in conversion of the reaction product to a final product of ~25.6 kDa (~21 kDa for the core protein and 4.4 kDa for [^{125}I]-IbTX-D19Y/Y36F) (Figure 3). However, the features of the cross-linked β1 subunit before *N*-glycanase treatment appear to depend on the nature of the cotransfected α subunit with which it is associated. In membranes expressing full-length hSlo1, β1 displays behavior identical to that previously observed with native smooth muscle Maxi-K channels (*18*). For Maxi-K_{1-343}, the β1 adduct displays a significantly higher molecular weight than that found after transfection with full-length hSlo1, suggesting a larger extent of glycosylation. However, a lower extent of glycosylation is seen with Maxi-K_{1-441} and Maxi-K_{1-651}. These differences in glycosylation patterns of β1 could be associated with the residence of the channel complex in different cellular compartments. Regardless of the mechanism, these results clearly indicate that the S_0-S_6 linker region of the channel is the only determinant for association of this moiety with the β1 subunit.

Cell Surface Expression of Maxi-K Channels. The results of Figure 3 concerning glycosylation patterns of β1 suggest differences in trafficking of the Maxi-K channel complexes. To assess the expression of each of these proteins at the cell surface, binding of [^{125}I]IbTX-D19Y/Y36F, or the fluorescence derivative, Alexa-Fluor488-IbTX, was carried out in intact cells after transient transfection of the respective constructs. The two probe peptides were first characterized with cells stably expressing the full-length Maxi-K channel. In these cells, binding of [^{125}I]IbTX-D19Y/Y36F is inhibited, in a dose-dependent manner, by IbTX and ChTX with IC_{50} values of 4.9 and 4.0 nM, respectively, and stimulated by the indole diterpene, paxilline (Figure 4A). Incubation of cells with Alexa-Fluor488-IbTX caused the appearance of a fluorescence signal that was also sensitive to the presence of either IbTX (Figure 4B,C) or paxilline (Figure 4D,E) in the incubation medium. All these data suggest that the interaction of the two IbTX peptide probes in intact cells reflects binding to Maxi-K channels expressed at the cell surface.

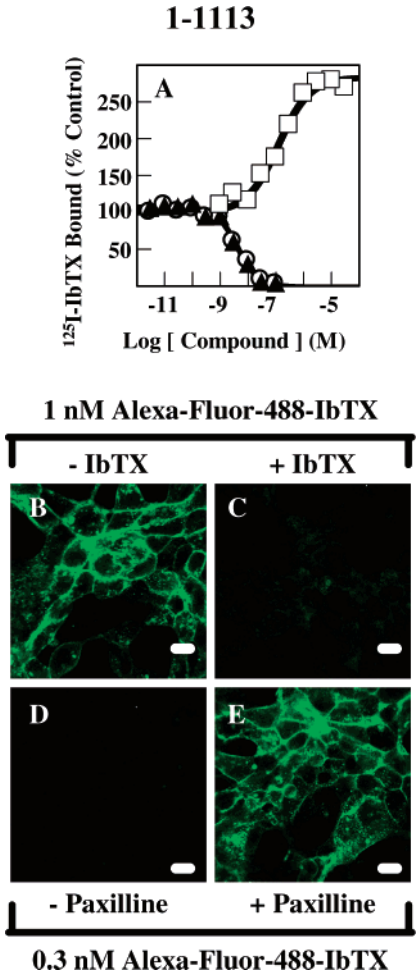

FIGURE 4: Binding of [^{125}I]IbTX-D19Y/Y36F or Alexa-Fluor488-IbTX to HEK293 cells stably transfected with Maxi-K_{1-1113} and β1. (A) HEK293 cells stably transfected with Maxi-K_{1-1113} and β1 were seeded in 96-well poly-D-lysine-coated plates, at a density of 40000 cells/well and incubated with ~60 pM [^{125}I]IbTX-D19Y/Y36F in the absence or presence of increasing concentrations of ChTX (○), IbTX (▲), or paxilline (□) for 4 h at 37 °C. Separation of bound from free ligand was carried out as indicated in Experimental Procedures. Specific binding data are plotted relative to those of an untreated control. (B−E) HEK293 cells stably transfected with Maxi-K_{1-1113} and β1 were incubated with 1 (B and C) or 0.3 nM Alexa-Fluor488-IbTX (D and E), in the absence (B and D) or presence of 200 nM IbTX (C) or 3 μM paxilline (E). Separation of bound from free ligand was carried out as described in Experimental Procedures. Images were obtained on a Zeiss LSM410 confocal imaging system with an argon laser tuned to 488 nm as an excitation source and 535/50 BP as the emission filter. The exposure time was the same in panels B−E. The scale bar is 10 μm.

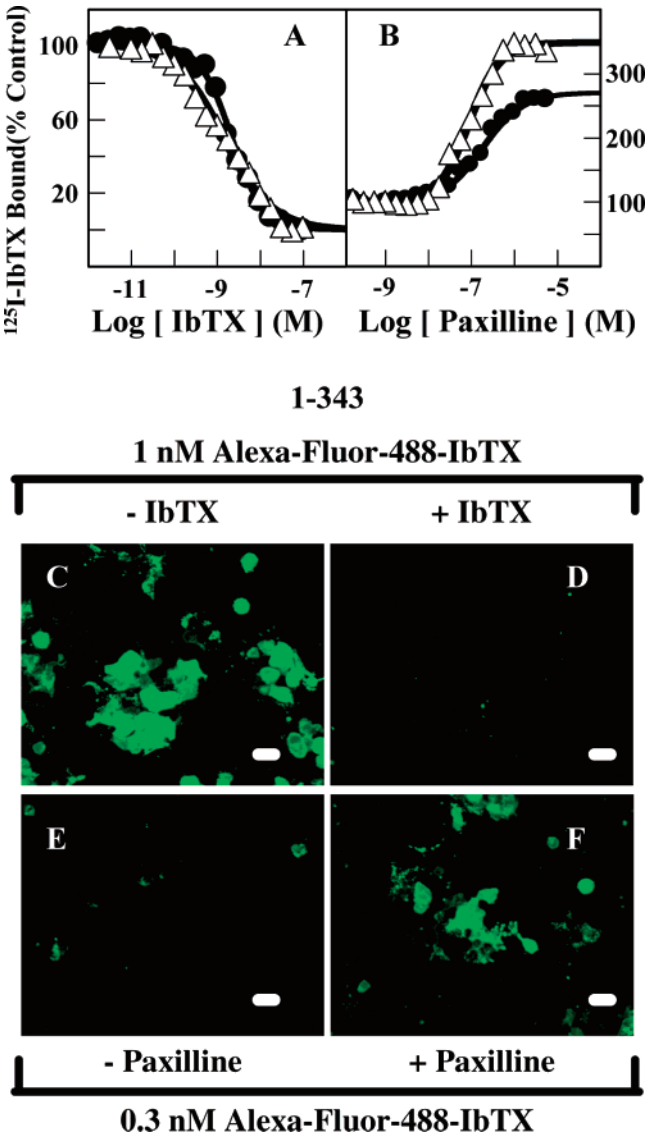

FIGURE 5: Binding of [^{125}I]IbTX-D19Y/Y36F or Alexa-Fluor488-IbTX to Maxi-K channels in intact cells. Role of the C-terminus. (A and B) TsA-201 cells transiently transfected with the β1 subunit and either Maxi-K_{1-343} (●), Maxi-K_{1-651}, or Maxi-K_{1-1113} (△) were incubated with ~60 pM [^{125}I]IbTX-D19Y/Y36F in the absence or presence of increasing concentrations of either IbTX (A) or paxilline (B). Specific binding data are presented relative to those of an untreated control. Specific binding of [^{125}I]IbTX-D19Y/Y36F was not detected in cells transfected with Maxi-K_{1-651}. (C−F) TsA-201 cells transiently transfected with Maxi-K_{1-343} and β1 were incubated with 1 (C and D) or 0.3 nM Alexa-Fluor488-IbTX (E and F), in the absence (C and E) or presence of 200 nM IbTX (D) or 3 μM paxilline (F). Separation of bound from free ligand was carried out as described in Experimental Procedures. Slides were sealed with #1 coverslips, and images were obtained on a Nikon TE300 instrument equipped with a 175 W xenon arc lamp and 403 ± 7 and 515 ± 15 nm filters. The exposure time was the same in panels C−F. The scale bar is 10 μm.

Binding of [^{125}I]IbTX-D19Y/Y36F was then evaluated in cells after transfection of the different Maxi-K channel constructs. Binding was not detected in cells transfected with Maxi-K_{1-323}. In cells expressing Maxi-K_{1-343} or Maxi-K_{1-441}, the characteristics of peptide binding were indistinguishable from those of the full-length protein (Figure 5A,B and data not shown). However, binding of [^{125}I]IbTX-D19Y/Y36F was not observed in cells expressing Maxi-K_{1-651}, under any conditions. Identical results were obtained using Alexa-Fluor488-IbTX (Figure 5C−F and data not shown). These data indicate that Maxi-K_{1-343} and Maxi-K_{1-441} are expressed at the cell surface, but Maxi-K_{1-651} is not. It appears that the Maxi-K_{1-651}−β1 complex is retained in intracellular compartment(s), and that tetramerization and association with β1 occur early on after protein biosynthesis.

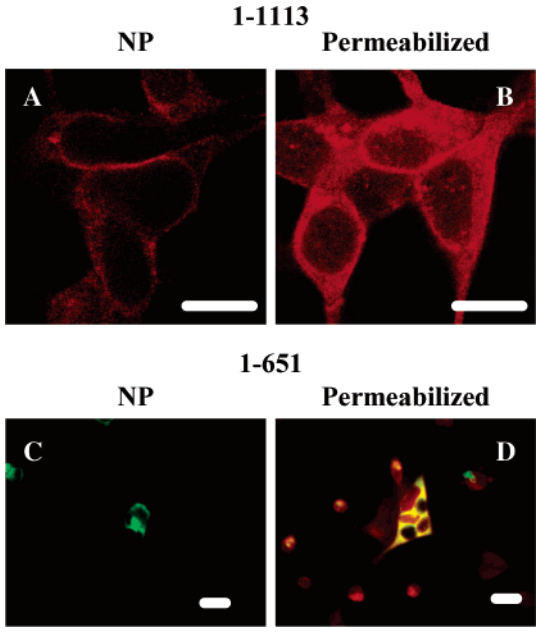

FIGURE 6: Immunostaining of Maxi-K channels in nonpermeabilized and permeabilized cells. HEK293 cells stably expressing Maxi-K_{1-1113} and β1 (A and B) or TsA-201 cells transiently transfected with Maxi-K_{1-651} and β1 (C and D) were fixed with 4% formaldehyde and incubated with crude polyclonal α28−40, directed against an extracellular epitope of hSlo1, before (A and C) or after (B and D) permeabilization with 0.2% Triton X-100. After being washed, cells were incubated with Alexa-Fluor546 goat anti-rabbit IgG, and images were obtained on a Zeiss LSM410 confocal imaging system or on a Nikon TE300 instrument. In nonpermeabilized Maxi-K_{1-1113} cells (A), labeling can be observed along the cell surface of the cells. In panels C and D, an ER marker encoded by pECFP-ER was also cotransfected. Cells expressing this protein are colored green, whereas cells expressing Maxi-K_{1-651} are colored red. The colocalization of these two proteins is shown in yellow. The scale bar is 10 μm.

Expression of the Maxi-K channel protein in cells was also assessed in immunocytochemistry experiments using an antibody raised against the N-terminal region of the channel. Because its epitope sequence is extracellular, the antibody can be used with nonpermeabilized cells to detect cell surface-expressed channels. Figure 6 presents immunofluorescence pictures of nonpermeabilized (A) and permeabilized (B) HEK293 cells stably transfected with the full-length Maxi-K protein. Under nonpermeabilized conditions, fluorescence localizes to the cell surface, whereas after permeabilization, a broader fluorescence staining can be seen throughout the cells. A similar staining pattern was observed with Maxi-K_{1-343} and Maxi-K_{1-441} (data not shown). In marked contrast, and in agreement with other results, cells transfected with Maxi-K_{1-651} only display a fluorescence signal after permeabilization (Figure 6C,D), and the protein appears to colocalize with an endoplasmic reticulum (ER) marker (Figure 6D). Results similar to those of Maxi-K_{1-651} were obtained with Maxi-K_{1-323} (data not shown).

Functional Expression of Truncated Constructs. Channel activity of Maxi-K channel constructs was evaluated in patch

clamp recordings of transiently transfected cells. In agreement with [^{125}I]IbTX-D19Y/Y36F binding experiments, transfection with Maxi-K_{1-323} did not yield functional Maxi-K channels in any recording configuration, on-cell ($n = 15$ and 16, without and with β1, respectively), whole-cell ($n = 6$ with β1), or inside-out ($n = 3$ with β1), over a wide range of calcium concentrations and membrane potentials. Although Maxi-K_{1-343} and Maxi-K_{1-441} are expressed at the cell surface and form tetramers, Maxi-K currents were not observed in whole-cell, on-cell, or excised patch recordings using these constructs, regardless of whether the β1 subunit had been cotransfected. For example, in experiments with Maxi-K_{1-343}, on-cell ($n = 15$ and 21, without and with β1, respectively), whole-cell ($n = 3$ and 16, without and with β1, respectively), and inside-out ($n = 12$ and 17, without and with β1, respectively) recordings were made.

Because Maxi-K_{1-651} is not expressed at the cell surface, it is not possible to determine whether this construct makes functional channels. However, cotransfection of cells with both Maxi-K_{1-651} and Maxi-$K_{652-1113}$ rescued the protein to the cell surface (Figure 7A−D) and, in agreement with previous data (*9*, *27*), also produced channels with properties identical to those of the full-length protein (Figure 7E−G). In inside-out patch recordings with 1 μM free calcium, the $V_{1/2}$ values of channel activation for Maxi-K_{1-651}/Maxi-$K_{652-1113}$ in the absence or presence of β1 (68.2 ± 3.3 and 42.5 ± 4.4 mV, respectively) were nearly identical to the values obtained with hSlo1 (68.2 ± 4.4 and 42.4 ± 4.6 mV, respectively) (Figure 7E,F) under the same experimental conditions, and channels were sensitive to calcium and the selective Maxi-K channel inhibitor paxilline (Figure 7G). In marked contrast, cotransfection of Maxi-K_{1-343} and its complement Maxi-$K_{344-1113}$ or cotransfection of Maxi-K_{1-441} and Maxi-$K_{442-1113}$ did not yield functional channels (data not shown). Although similar levels of [^{125}I]IbTX-D19Y/Y36F binding sites were detected in intact cells, inside-out recordings of hSlo1 (five of five cells) or Maxi-K_{1-651}/Maxi-$K_{652-1113}$ (13 of 14 cells) yielded Maxi-K currents of >1 nA at 70 mV, and no detectable Maxi-K currents were observed at 200 mV with either Maxi-K_{1-343}/Maxi-$K_{344-1113}$ ($n = 12$) or Maxi-K_{1-441}/Maxi-$K_{442-1113}$ ($n = 11$).

DISCUSSION

The results presented in this study using different Maxi-K channel C-terminal constructs (Figure 1 and Table 1) demonstrate that the S_0-S_6 linker domain of hSlo1, comprising the first 343 residues of the protein, is sufficient for channel tetramerization, interaction with the β1 subunit, and cell surface expression, and that the two RCK domains of hSlo1, containing residues 344−1113, are not necessary for these functions, but play a critical role in channel function (Table 1). These conclusions were derived from the use, for the first time, of a number of techniques that directly and unambiguously define those parameters. In addition to monitoring tetramer formation, the two selective Maxi-K channel peptide inhibitors employed in this study provide a more direct and quantitative alternative for characterizing channels present at the cell surface than another approach commonly used, which consists of biotinylation of cell surface proteins, followed by immunoprecipitation and immunostaining. It is interesting that Maxi-K_{1-651}, despite tetramerization and association with β1, appears to be fully

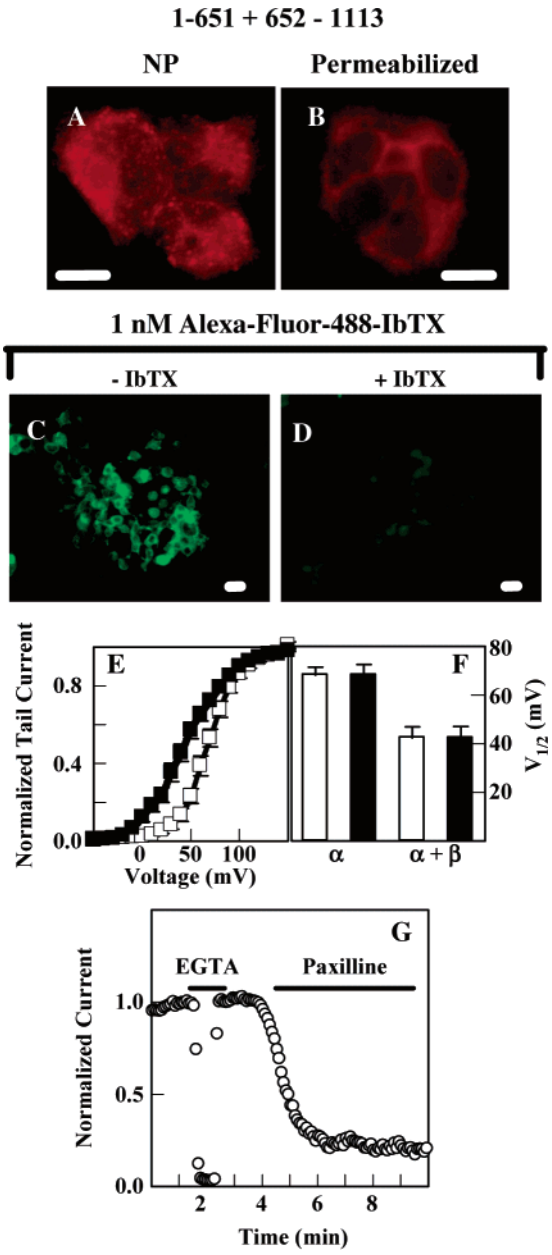

FIGURE 7: C-Terminal RCK2 domain rescues Maxi-K_{1-651} to the cell surface. TsA-201 cells transiently cotransfected with Maxi-K_{1-651} and Maxi-$K_{652-1113}$ were immunostained with α28−40 before (A) or after (B) permeabilization with 0.2% Triton X-100 or incubated with 1 nM Alexa-Fluor488-IbTX, in the absence (C) or presence (D) of 200 nM IbTX. Images were obtained as indicated above. The exposure time was the same in panels C and D. The scale bar is 10 μm. In transfections with both Maxi-K_{1-651} and Maxi-$K_{652-1113}$, Maxi-K channels with characteristics identical to those of the full-length channel protein were observed in inside-out patches in the presence of 1 μM free calcium (E−G). Conductance−voltage curves are shown for cotransfection of Maxi-K_{1-651} and Maxi-$K_{652-1113}$, in the absence (□) or presence (■) of β1 subunit (E). The $V_{1/2}$ for channel activation, in the absence or presence of β1, is identical for hSlo1 [white bars; 68.2 ± 4.4 ($n = 8$) and 42.4 ± 4.6 ($n = 7$), respectively] and Maxi-K_{1-651} and Maxi-$K_{652-1113}$ channels [black bars; 68.2 ± 3.3 ($n = 8$) and 42.5 ± 4.4 ($n = 11$), respectively] (F). Channels due to Maxi-K_{1-651} and Maxi-$K_{652-1113}$ were sensitive to removal of intracellular calcium (application of EGTA) and low concentrations (30 nM) of paxilline (G). When transfections of Maxi-K_{1-651} were carried out in the absence of Maxi-$K_{652-1113}$, neither binding of Alexa-Fluor488-IbTX nor channel activity was detected.

Table 1: Characteristics of the Different Maxi-K Channel Constructs Cotransfected with the β1 Subunit, in Terms of Channel Tetramerization ([^{125}I]IbTX binding to membranes), Cell Surface Expression (IbTX binding to intact cells; immunostaining in nonpermeabilized cells with an antibody directed against an extracellular epitope), and Maxi-K Channel Function (electrophysiology)

	Maxi-K_{1-323}	Maxi-K_{1-343}	Maxi-K_{1-441}	Maxi-K_{1-651}	Maxi-K_{1-1113}
[^{125}I]IbTX binding (membranes)	no	yes	yes	yes	yes
IbTX binding (cells)	no	yes	yes	no yes[c]	yes
immunostaining nonpermeabilized/permeabilized	no/yes	yes/yes	yes/yes	no/yes yes/yes[c]	yes/yes
channel activity	no	no no[a]	no no[b]	no yes[c]	yes

[a] When cotransfected with Maxi-$K_{344-1113}$. [b] When cotransfected with Maxi-$K_{442-1113}$. [c] When cotransfected with Maxi-$K_{652-1113}$.

retained in intracellular organelles. Because other regions of the protein, in addition to the outer channel vestibule, appear to be properly folded based on the data obtained with indole diterpenes, these data suggest that, at least for Maxi-K_{1-651}, the mechanisms that control its trafficking are not related to quality control of the protein and may involve specific conformations of the C-terminal domain of hSlo1. This idea is consistent with cell surface expression observed upon cotransfection of Maxi-K_{1-651} with Maxi-$K_{652-1113}$. The fact that others have identified regions in the RCK domains necessary for either channel tetramerization (*13*) or cell surface expression (*15*, *16*) can be reconciled with these data if those channel constructs behaved as Maxi-K_{1-651} did. Our data with Maxi-K_{1-651} are also consistent with previous data (*9*, *27*) describing expression of functional channels by coexpression of two adjacent sections of the protein, and with the structure of the bacterial calcium-activated potassium channel, MthK, in which the cytoplasmic gating ring is formed by the association of eight RCK domains, one from each of the pore-forming subunits and four from the intracellular solution (*10*). The mechanisms responsible for lack of cell surface expression of Maxi-K_{1-651} are not well understood. Inspection of the Maxi-K amino acid region of residues 451−651 does not reveal the presence of retention/retrieval sequences that have been characterized as altering trafficking in other proteins (*32*, *33*). Dibasic motifs are present near the carboxyl terminus, but their role in Maxi-K_{1-651} trafficking needs to be explored. In any event, these same motifs and others are also present in Maxi-K_{1-1113}, and if relevant for channel trafficking, these motifs will have to be masked to account for the cell surface expression of this construct.

Despite abundant cell surface expression, both Maxi-K_{1-343} and Maxi-K_{1-441} constructs did not yield functional channels, and channel activity was not detected after coexpression with their respective C-terminal regions, Maxi-$K_{344-1113}$ and Maxi-$K_{442-1113}$. These data are consistent with the proposed role for the linker-gating ring in channel gating, and suggest that the RCK1 domain must exist covalently attached to the linker to be able to transmit the energy necessary for opening the channel.

Contrary to previous results (*17*), functional channels were not observed with Maxi-K_{1-323} in this study, under several different recording conditions, over a wide range of calcium concentrations and membrane potentials. Given the intracellular retention of the protein observed in this study, and in a previous study (*14*), the lack of evidence for channel tetramerization using a highly sensitive detection system (this study), and the truncated channel's decreased half-life compared with that of hSlo1 (*14*), the expectations for functional activity of this construct should be low. We do not know about the probability of channel detection in the other study (*17*), but the possibility remains that the Maxi-K channels observed might be endogenous to the host system, rather than representing the consequence of Maxi-K_{1-323} expression. Alternatively, the cell could have provided a complementary C-terminal region, as occurs in bacteria, although in this case the first RCK domain is covalently bound to the pore region and only the second RCK domain comes from the cytoplasm.

Two other aspects of Maxi-K channel function should be mentioned. One concerns the site of action of pharmacological agents other than the pore-blocking peptides. In this context, the results with the selective indole diterpene Maxi-K channel blockers suggest that these molecules exert their action by binding to a site present within the S_0-S_6 linker region of the channel. Given the allosteric interaction between the extracellular binding sites for peptides and indole diterpenes, which block at a site accessible from the intracellular surface (*8*, *30*), it is possible that the indole diterpenes bind in the water-filled cavity beneath the selectivity filter. Second, the interaction of hSlo1 with the β1 subunit is also determined by the first 343 residues of the protein. The characteristics of β1, with two transmembrane domains, a large extracellular loop, and short N- and C-terminal regions, suggest that helical interactions between α and β1 subunits are likely to occur in the complex. In this context, it has previously been shown that S_0 of hSlo1 is required for the functional effects of β1 (*31*). Whatever the topological arrangement of the subunits is, this must bring the extracellular loop of β very close to the pore, an idea that is supported by a large body of experimental data, including cross-linking experiments (*34*−*36*).

The contribution of a given ion channel to cell physiology is governed by many factors that occur after protein biosynthesis. A decrease in the level of cell surface expression of Maxi-K channels in mouse myometrium at the end of pregnancy has been proposed to contribute to preparation of myometrium for delivery (*37*). This reduction in the protein level appears to be due to altered channel trafficking under the control of sex hormones during pregnancy, since high levels of the protein can be seen localized in perinuclear organelles at the end of pregnancy. Understanding mechanisms that control protein trafficking could therefore have importance in attempting to modulate ion channel function for therapeutic benefit.

In this study, we have used a combination of newly developed techniques and protocols to assess formation and

surface expression of Maxi-K channel constructs with the goal of identifying regions of the channel necessary for functional channel expression. The results indicate that the channel domain ranging from the N-terminus through the S_6 linker region contains the determinants necessary for formation and surface expression of tetramers, while the C-terminal domain is needed for normal channel gating and can also affect surface expression.

ACKNOWLEDGMENT

We thank Drs. James Herrington and Birgit Priest for important discussions during the course of this work, Paul Fischer for assistance with the Zeiss LSM410 instrument, and Neil Mehrotra for technical assistance.

REFERENCES

1. Wickenden, A. (2002) K^+ channels as therapeutic drug targets, *Pharmacol. Ther. 94*, 157−182.
2. Bendahhou, S., Donaldson, M. R., Plaster, N. M., Tristani Firouzi, M., Fu, Y. H., and Ptacek, L. J. (2003) Defective potassium channel Kir2.1 trafficking underlies Andersen-Tawil syndrome, *J. Biol. Chem. 278*, 51779−51785.
3. Manganas, L. N., Akhtar, S., Antonucci, D. E., Campomanes, C. R., Dolly, J. O., and Trimmer, J. S. (2001) Episodic ataxia type-1 mutations in the Kv1.1 potassium channel display distinct folding and intracellular trafficking properties, *J. Biol. Chem. 276*, 49427−49434.
4. Huopio, H., Shyng, S. L., Otonkoski, T., and Nichols, C. G. (2002) K(ATP) channels and insulin secretion disorders, *Am. J. Physiol. 283*, E207−E216.
5. Thomas, D., Kiehn, J., Katus, H. A., and Karle, C. A. (2003) Defective protein trafficking in hERG-associated hereditary long QT syndrome (LQT2): Molecular mechanisms and restoration of intracellular protein processing, *Cardiovasc. Res. 60*, 235−241.
6. Orio, P., Rojas, P., Ferreira, G., and Latorre, R. (2002) New disguises for an old channel: MaxiK channel β-subunits, *News Physiol. Sci. 17*, 156−161.
7. McManus, O. B., Helms, L. M., Pallanck, L., Ganetzky, B., Swanson, R., and Leonard, R. J. (1995) Functional role of the β subunit of high conductance calcium-activated potassium channels, *Neuron 14*, 645−650.
8. Hanner, M., Schmalhofer, W. A., Munujos, P., Knaus, H. G., Kaczorowski, G. J., and Garcia, M. L. (1997) The β subunit of the high-conductance calcium-activated potassium channel contributes to the high-affinity receptor for charybdotoxin, *Proc. Natl. Acad. Sci. U.S.A. 94*, 2853−2858.
9. Meera, P., Wallner, M., Song, M., and Toro, L. (1997) Large conductance voltage- and calcium-dependent K^+ channel, a distinct member of voltage-dependent ion channels with seven N-terminal transmembrane segments (S0−S6), an extracellular N terminus, and an intracellular (S9−S10) C terminus, *Proc. Natl. Acad. Sci. U.S.A. 94*, 14066−14071.
10. Jiang, Y., Lee, A., Chen, J., Cadene, M., Chait, B. T., and MacKinnon, R. (2002) Crystal structure and mechanism of a calcium-gated potassium channel, *Nature 417*, 515−522.
11. Jiang, Y., Pico, A., Cadene, M., Chait, B. T., and MacKinnon, R. (2001) Structure of the RCK domain from the *E. coli* K^+ channel and demonstration of its presence in the human BK channel, *Neuron 29*, 593−601.
12. Niu, X., Qian, X., and Magleby, K. L. (2004) Linker-gating ring complex as passive spring and Ca^{2+}-dependent machine for a voltage- and Ca^{2+}-activated potassium channel, *Neuron 42*, 745−756.
13. Quirk, J. C., and Reinhart, P. H. (2001) Identification of a novel tetramerization domain in large conductance K_{Ca} channels, *Neuron 32*, 13−23.
14. Bravo Zehnder, M., Orio, P., Norambuena, A., Wallner, M., Meera, P., Toro, L., Latorre, R., and Gonzalez, A. (2000) Apical sorting of a voltage- and Ca^{2+}-activated K^+ channel α-subunit in Madin-Darby canine kidney cells is independent of N-glycosylation, *Proc. Natl. Acad. Sci. U.S.A. 97*, 13114−13119.
15. Wang, S. X., Ikeda, M., and Guggino, W. B. (2003) The cytoplasmic tail of large conductance, voltage- and Ca^{2+}-activated K^+ (MaxiK) channel is necessary for its cell surface expression, *J. Biol. Chem. 278*, 2713−2722.
16. Kwon, S.-H., and Guggino, W. B. (2004) Multiple sequences in the C terminus of MaxiK channels are involved in expression, movement to the cell surface, and apical localization, *Proc. Natl. Acad. Sci. U.S.A. 101*, 15237−15242.
17. Piskorowski, R., and Aldrich, R. W. (2002) Calcium activation of BK(Ca) potassium channels lacking the calcium bowl and RCK domains, *Nature 420*, 499−502.
18. Koschak, A., Koch, R. O., Liu, J., Kaczorowski, G. J., Reinhart, P. H., Garcia, M. L., and Knaus, H. G. (1997) [^{125}I]Iberiotoxin-D19Y/Y36F, the first selective, high specific activity radioligand for high-conductance calcium-activated potassium channels, *Biochemistry 36*, 1943−1952.
19. Pragl, B., Koschak, A., Trieb, M., Obermair, G., Kaufmann, W. A., Gerster, U., Blanc, E., Hahn, C., Prinz, H., Schutz, G., Darbon, H., Gruber, H. J., and Knaus, H. G. (2002) Synthesis, characterization, and application of cy-dye- and alexa-dye-labeled hongotoxin(1) analogues. The first high affinity fluorescence probes for voltage-gated K^+ channels, *Bioconjugate Chem. 13*, 416−425.
20. Wallner, M., Meera, P., Ottolia, M., Kaczorowski, G. J., Latorre, R., Garcia, M. L., Stefani, E., and Toro, L. (1995) Characterization of and modulation by a β-subunit of a human maxi KCa channel cloned from myometrium, *Recept. Channels 3*, 185−199.
21. Hanner, M., Green, B., Gao, Y. D., Schmalhofer, W. A., Matyskiela, M., Durand, D. J., Felix, J. P., Linde, A. R., Bordallo, C., Kaczorowski, G. J., Kohler, M., and Garcia, M. L. (2001) Binding of correolide to the $K_v1.3$ potassium channel: Characterization of the binding domain by site-directed mutagenesis, *Biochemistry 40*, 11687−11697.
22. Giangiacomo, K. M., Fremont, V., Mullmann, T. J., Hanner, M., Cox, R. H., and Garcia, M. L. (2000) Interaction of charybdotoxin S10A with single maxi-K channels: Kinetics of blockade depend on the presence of the β1 subunit, *Biochemistry 39*, 6115−6122.
23. Knaus, H. G., Eberhart, A., Koch, R. O., Munujos, P., Schmalhofer, W. A., Warmke, J. W., Kaczorowski, G. J., and Garcia, M. L. (1995) Characterization of tissue-expressed α subunits of the high conductance Ca^{2+}-activated K^+ channel, *J. Biol. Chem. 270*, 22434−22439.
24. Hamill, O. P., Marty, A., Neher, E., Sakmann, B., and Sigworth, F. J. (1981) Improved patch-clamp techniques for high-resolution current recording from cells and cell-free membrane patches, *Pfluegers Arch. 391*, 85−100.
25. Xia, X. M., Zeng, X., and Lingle, C. J. (2002) Multiple regulatory sites in large-conductance calcium-activated potassium channels, *Nature 418*, 880−884.
26. Xia, X. M., Zhang, X., and Lingle, C. J. (2004) Ligand-dependent activation of Slo family channels is defined by interchangeable cytosolic domains, *J. Neurosci. 24*, 5585−5591.
27. Wei, A., Solaro, C., Lingle, C., and Salkoff, L. (1994) Calcium sensitivity of BK-type KCa channels determined by a separable domain, *Neuron 13*, 671−681.
28. Schreiber, M., Yuan, A., and Salkoff, L. (1999) Transplantable sites confer calcium sensitivity to BK channels, *Nat. Neurosci. 2*, 416−421.
29. MacKinnon, R. (1991) Determination of the subunit stoichiometry of a voltage-activated potassium channel, *Nature 350*, 232−235.
30. Knaus, H. G., McManus, O. B., Lee, S. H., Schmalhofer, W. A., Garcia Calvo, M., Helms, L. M., Sanchez, M., Giangiacomo, K., Reuben, J. P., Smith, A. B., III, et al. (1994) Tremorgenic indole alkaloids potently inhibit smooth muscle high-conductance calcium-activated potassium channels, *Biochemistry 33*, 5819−5828.
31. Tanaka, Y., Koike, K., Alioua, A., Shigenobu, K., Stefani, E., and Toro, L. (2004) β1-subunit of MaxiK channel in smooth muscle: A key molecule which tunes muscle mechanical activity, *J. Pharmacol. Sci. 94*, 339−347.
32. Teasdale, R. D., and Jackson, M. R. (1996) Signal-mediated sorting of membrane proteins between the endoplasmic reticulum and the Golgi apparatus, *Annu. Rev. Cell Dev. Biol. 12*, 27−54.
33. Zarei, M. M., Eghbali, M., Alioua, A., Song, M., Knaus, H.-G., Stefani, E., and Toro, L. (2004) An endoplasmic reticulum trafficking signal prevents surface expression of a voltage- and Ca^{2+}-activated K^+ channel splice variant, *Proc. Natl. Acad. Sci. U.S.A. 101*, 10072−10077.
34. Munujos, P., Knaus, H. G., Kaczorowski, G. J., and Garcia, M. L. (1995) Cross-linking of charybdotoxin to high-conductance calcium-activated potassium channels: Identification of the co-

valently modified toxin residue, *Biochemistry 34*, 10771−10776.
35. Garcia Calvo, M., Knaus, H. G., McManus, O. B., Giangiacomo, K. M., Kaczorowski, G. J., and Garcia, M. L. (1994) Purification and reconstitution of the high-conductance, calcium-activated potassium channel from tracheal smooth muscle, *J. Biol. Chem. 269*, 676−682.
36. Meera, P., Wallner, M., and Toro, L. (2000) A neuronal β subunit (KCNMB4) makes the large conductance, voltage- and Ca^{2+}-activated K^+ channel resistant to charybdotoxin and iberiotoxin, *Proc. Natl. Acad. Sci. U.S.A. 97*, 5562−5567.
37. Eghbali, M., Toro, L., and Stefani, E. (2003) Diminished surface clustering and increased perinuclear accumulation of large conductance Ca^{2+}-activated K^+ channel in mouse myometrium with pregnancy, *J. Biol. Chem. 278*, 45311−45317.

BI050527U